

## Model for the structural changes occurring at low temperatures in PdD<sub>x</sub>

O. Blaschko, P. Fratzl, and R. Klemencic

*Institut für Experimentalphysik der Universität Wien, Strudlhofgasse 4, 1090 Wien, Austria*

*and Physikinstitut, Forschungszentrum Seibersdorf, 2444 Seibersdorf, Austria*

(Received 6 February 1981)

A structural model for the short-range-ordered state in PdD<sub>x</sub>, with  $0.7 < x \leq 0.78$ , observed at low temperatures, is proposed. The model describes the complicated diffuse intensity contours with "mixed" microdomains consisting of cells of the Ni<sub>4</sub>Mo type. A simple distortion, i.e., a relaxation of the D atoms towards vacant sites, is introduced in the "mixed" microdomain and accounts for the measured intensity asymmetry. Furthermore, a measurement of the intensities of the superlattice reflections in the long-range-ordered Ni<sub>4</sub>Mo structure is presented, and its result is reproduced by calculation, when the same relaxation towards the vacancy, is assumed. Finally an important Debye-Waller factor for the superlattice reflections is found.

### I. INTRODUCTION

Phase diagrams of metal-hydrogen systems generally show phases where the hydrogen is ordered on its interstitial sublattice. In PdD<sub>x</sub> only recently experimental evidence has been obtained for the existence at low temperatures of an ordered state of D.<sup>1,3</sup>

Neutron diffraction investigations have shown, in a temperature region corresponding to the region of the "50-K anomaly," a drastic increase of short-range order of D on octahedral interstitial sites.<sup>2,3</sup> The short-range order, for all concentrations between  $x = 0.63$  and  $0.78$ , is characterized by a broad diffuse intensity around the  $(1, \frac{1}{2}, 0)$  reciprocal-lattice point and its shape depends rather strongly on concentration. At lower concentrations, i.e.,  $x \leq 0.68$  the diffuse intensity is centered around the  $(1, \frac{1}{2}, 0)$  point<sup>2</sup> but at higher concentrations the intensity distribution shows, in the vicinity of the  $(1, \frac{1}{2}, 0)$  point, maxima whose positions cannot be described by simple rational numbers; e.g., a maximum observed in PdD<sub>0.75</sub> is located at  $(1.14, 0.48, 0)$ . Moreover, the intensity distribution is asymmetric with respect to a (100) reciprocal plane; i.e., the intensities at reciprocal-lattice points  $(h, k, l)$  for  $h < 1$  are in the order of 30% lower for all concentrations.<sup>3</sup> Furthermore, for  $x > 0.76$  after some aging time, a superlattice reflection appears at the  $(\frac{4}{5}, \frac{2}{5}, 0)$  point and increases in intensity whereas the broad diffuse distribution disappears. This  $(\frac{4}{5}, \frac{2}{5}, 0)$  superlattice reflection shows the presence of a long-range-ordered D phase described by an interstitial Ni<sub>4</sub>Mo structure.<sup>1,3</sup>

The long-range-ordered Ni<sub>4</sub>Mo structure corresponds to an ordering process of D on (420) planes, where four consequent (420) planes are filled with D and the fifth is vacant. The short-range order inten-

sity has also been ascribed to ordering of D on (420) planes in microdomains,<sup>3</sup> but no structural model has been proposed for the microdomains responsible for the complicated shape and for the intensity asymmetry of the iso-intensity contours observed experimentally in PdD<sub>x</sub>, with  $x$  from  $0.71$  to  $0.78$ .

In the present communication we propose a structural model for the short-range-ordered state in PdD<sub>x</sub>, with  $x$  from  $0.71$  to  $0.78$ . Conceptually the model starts from some ideas on a mixed state of ordered microdomains, which have been put forward in a recent publication.<sup>3</sup> In Sec. II, we show the structure of microdomains which are able to describe the observed intensity pattern and we introduce a simple distortion of the D sublattice which accounts for the observed intensity asymmetry.

In Sec. III we present an experimental investigation of superlattice reflections in the long-range-ordered Ni<sub>4</sub>Mo structure and we show that the results can be explained by the distortion field introduced in Sec. II.

### II. MODEL FOR THE SHORT-RANGE-ORDERED STATE

Ordering on (420) planes has been discussed by Okamoto and Thomas<sup>4</sup> for the Ni-Mo system and more generally by de Fontaine.<sup>5</sup> In Ni-Mo a short-range-order intensity appears at the  $(1, \frac{1}{2}, 0)$  and the formation of the long-range-ordered Ni<sub>4</sub>Mo structure (Strukturbericht symbol *D1a*) is revealed by the observation of a superlattice reflection at the  $(\frac{4}{5}, \frac{2}{5}, 0)$  point. Both authors describe the short-range-ordered state by "partially ordered" microdomains with the Ni<sub>3</sub>Mo structure (Strukturbericht symbol *DO*<sub>22</sub>) creating intensity at the  $(1, \frac{1}{2}, 0)$  point.

For PdD<sub>x</sub> a simple analogy with the Ni-Mo system

is not adequate as the diffuse intensity in the vicinity of the  $(1, \frac{1}{2}, 0)$  point has a complicated shape and shows maxima outside the  $(1, \frac{1}{2}, 0)$  point.

De Fontaine has pointed out that different ordering possibilities may appear in the ordering on (420) planes.<sup>5</sup> For PdD<sub>x</sub> these ordering possibilities can be described by the following structures:

(a) Two (420) planes filled with D and two (420) planes with vacant interstitial sites, corresponding to a 50 at. % D concentration and producing intensity at the  $(1, \frac{1}{2}, 0)$  point.

(b) Two (420) planes filled with D and one vacant, corresponding to a 67 at. % D concentration and producing intensity at the  $(\frac{4}{3}, \frac{2}{3}, 0)$  point.

(c) Three (420) planes filled with D and one vacant, corresponding to a 75 at. % concentration and producing intensity at the  $(1, \frac{1}{2}, 0)$  and the  $(1, 0, 0)$  point.

(d) Four (420) planes filled with D and one vacant, corresponding to 80 at. % D and producing intensity at the  $(\frac{4}{5}, \frac{2}{5}, 0)$  point.

For the concentration range under investigation in PdD<sub>x</sub>, i.e.,  $0.7 < x \leq 0.78$ , microdomains correspond-

ing to the structures described above in (b), (c), and (d) should be the most favored. (Figure 1 shows these structures.) Each structure alone cannot account for the observed experimental facts, but the structures have some similarity and locally their unit cells can be transformed mutually into each other by simply exchanging one or two filled and vacant sites.

The simple transformation between the different structures, as a result of a few diffusive D jumps, may favor a short-range-ordered state produced by an "ensemble" of microdomains, where each domain consists of differently ordered cells with the structure described above. Many such microdomains can be constructed by arranging the unit cells of Fig. 1 like "mosaic stones." Two examples for the composition of such a "mixed" domain are shown in Fig. 2. The observed short-range-order intensity around the  $(1, \frac{1}{2}, 0)$  point may therefore be produced by the contribution of many "mixed" structures. The occurrence in the composed domain of the individual ordering possibilities should depend on the overall D concentration of the crystal. The diffracted intensity by each composed domain is characterized by the Bragg intensities of the corresponding "mixed struc-

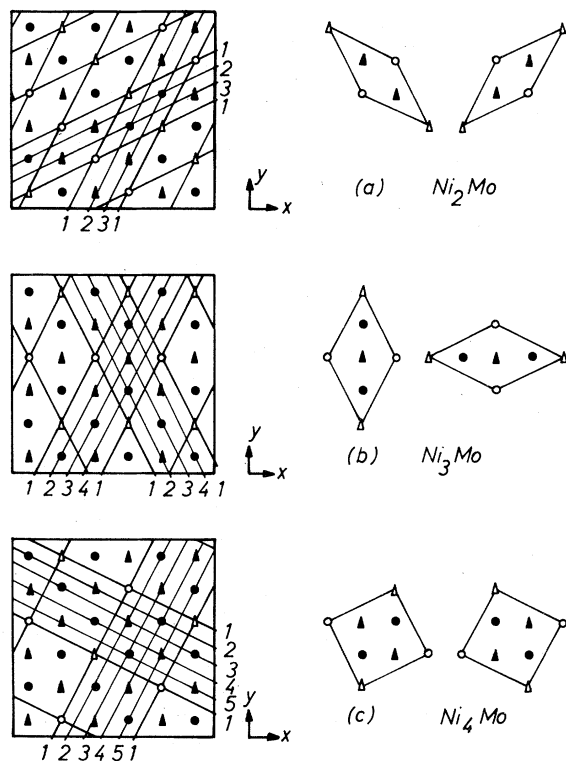


FIG. 1. Projection on a (001) plane of the structure and the unit cell for the (a) Ni<sub>2</sub>Mo, (b) Ni<sub>3</sub>Mo, (c) Ni<sub>4</sub>Mo superstructures of the fcc lattice. Filled symbols represent D atoms, open symbols vacancies; circles are corresponding to level 0 and triangles to level  $\frac{1}{2}$ .

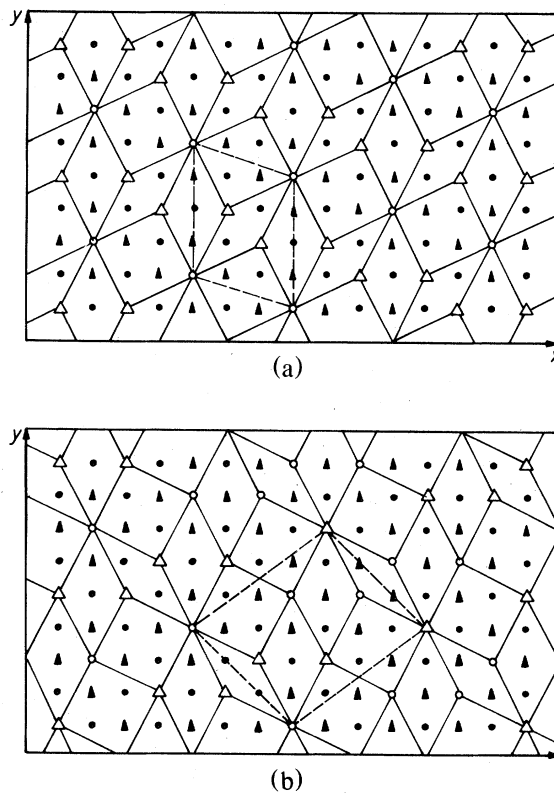


FIG. 2. Examples of mixed microdomains constructed with Ni<sub>n</sub>Mo "mosaic stones." The unit cell of the structure is depicted by broken line. The unit cell contains (a) 12 fcc sites and 9 D atoms; (b) 21 fcc sites and 16 D atoms.

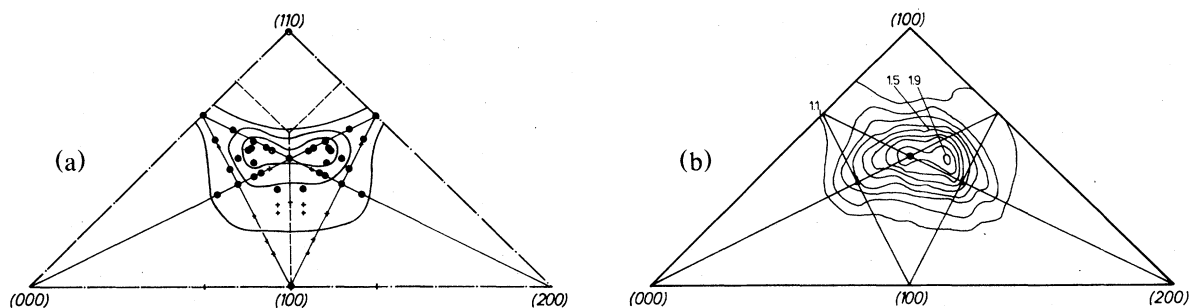


FIG. 3. (a) Calculated reflections for a number of mixed structures and isointensity contours. All valuable reflections occurring in this triangle for the considered structures are represented. + means half intensity of •. (b) Measured diffuse intensity distribution near the  $(1, \frac{1}{2}, 0)$  point in  $\text{PdD}_{0.75}$  (Ref. 3).

ture," which have been calculated. Figure 3(a) shows the results of 20 different domains, constructed similarly to those depicted in Fig. 2, with an average D concentration of 75 at.%. Figure 3(a) shows all reflections occurring within the depicted triangle. The figure shows the presence of intensity away from the  $(1, \frac{1}{2}, 0)$  point, with an accumulation of reflections in a region near a  $(1.15, 0.5, 0)$  point. Possible intensity contours of such a distribution of reflections from an "ensemble" of mixed domains are drawn and the results are in rather good agreement with the experimental facts<sup>3</sup> [Fig. 3(b)]. The measured intensity contours<sup>3</sup> show some concentration dependence, which can qualitatively be reproduced by composing the "mixed domains" in a way to obtain for the "ensemble" of all domains an average concentration consistent with the macroscopic one.

The calculated results of Fig. 3 are still symmetric with respect to a (100) plane, in contradiction to the experimental results, where the intensities on the left-hand side of the figure are lower by 30%.

By introducing a distortion in the "mixed" domains, i.e., the D-atom neighbors of the vacancy are shifted by  $\sim 1\%$  of the lattice parameter towards the vacant site, an intensity asymmetry similar to the experimental results can be obtained.

If D atoms have vacancies in their first neighborhood, this should break the equilibrium of the D-D interactions and local distortions can be expected. Each D atom has 12 nearest neighbors. Let  $\vec{d}_i (i=1, 12)$  be the unit vectors pointing from an origin at the D atom towards its nearest neighbors. If  $\sigma(i) (i=1, \dots, 12)$  is the site occupation operator [ $\sigma(i)=1$  if there is a D atom at the site  $i$ , =0 otherwise], the local symmetry will be respected if the distortion has the direction  $\vec{d}$  defined by

$$\vec{d} = \sum_{i=1}^{12} [1 - \sigma(i)] \vec{d}_i .$$

$\vec{d}$  is, within the symmetrization, directed towards the

nearest-neighbor vacancies. The displacement of the atom will be  $\epsilon \vec{d}$ . If  $\epsilon > 0$  it is a shift toward the vacancies, if  $\epsilon < 0$  in the inverse direction.

The atomic displacements in the unit cell and the resulting structure factors have been determined for the structures reported on Fig. 3(a) with different values of  $\epsilon$ . Calculations for  $\epsilon = +0.05 \text{ \AA}$  showed that for  $h < 1$  the intensities were in the order of 30% lower than for  $h > 1$  which is a good description of the experimental result. For  $\epsilon < 0$  the inverse effect (intensities higher for  $h < 1$ ) has been observed. This may indicate that the asymmetry with regards to the (100) plane<sup>3</sup> can be interpreted by a simple relatively small distortion, respecting the local symmetry and directed towards the vacant planes.

### III. LONG-RANGE-ORDERED STATE

#### A. Measurement of superlattice reflections

The intensities of the superlattice reflections of the interstitial  $\text{Ni}_4\text{Mo}$  phase were measured in  $\text{PdD}_{0.78}$ . The measurements were done on a conventional triple axis spectrometer at a 8-MW swimming-pool reactor. As monochromator a Zn(002) crystal was mounted and a Ge(111) crystal was used as analyzer to suppress the second-order contamination. The collimations were  $30'$  and the incident neutron wavelength was  $1 \text{ \AA}$ . As a sample a cylindrical single crystal of  $\text{PdD}_{0.78}$  was mounted into a cryostat and cooled down to 75 K. After 50 h at 75 K the  $(\frac{4}{5}, \frac{2}{5}, 0)$  superlattice reflections were well developed and the temperature was then lowered to 10 K.

Due to the lower symmetry of the tetragonal structure the  $\text{Ni}_4\text{Mo}$  phase appears in six variants. The superlattice reflections  $(\frac{4}{5}, \frac{2}{5}, 0)$  and  $(-\frac{4}{5}, \frac{2}{5}, 0)$  are representatives of the two different variants which can be observed in the plane  $l=0$ . The intensities of the superlattice reflections were measured along

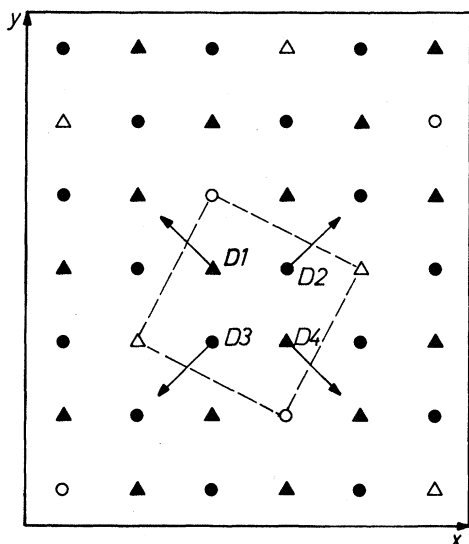


FIG. 4.  $\text{Ni}_4\text{Mo}$  structure is represented with the same conventions as in Fig. 1. Broken line shows a unit cell and the vector  $\vec{d}$  is represented by an arrow for the 4 atoms (D1–D4) in this unit cell. Calculation of  $\vec{d}$  is done in Table I.

several crystallographic directions of the tetragonal unit cell in two variants. No noticeable difference between equivalent reflections in the two variants has been observed.

#### B. Distortion field of the $\text{Ni}_4\text{Mo}$ structure

The structure factors for the  $(\frac{4}{5}, \frac{2}{5}, 0)$  and the  $(\frac{6}{5}, \frac{2}{5}, 0)$  reflections should be equal. However, as already found in Ref. 3 the  $(\frac{6}{5}, \frac{2}{5}, 0)$  is higher than the  $(\frac{4}{5}, \frac{2}{5}, 0)$  peak by a factor 2. This experimental fact can be reproduced by the calculation, when a distortion similar to that found in Sec. II is introduced in the perfect interstitial  $\text{Ni}_4\text{Mo}$  structure, i.e., D-atom neighbors of the vacancies are shifted towards the vacancy.

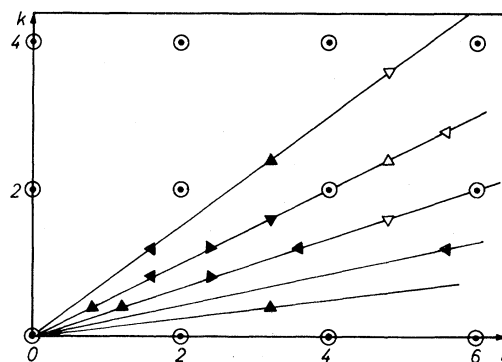


FIG. 5. In (001) reciprocal plane of fcc lattice (O represents Bragg reflections of Pd) are reported the measured points of  $\text{Ni}_4\text{Mo}$  superlattice reflections by a filled triangle. Open triangles indicate a nearly vanishing of structure factors which has been experimentally verified.

The vector  $\vec{d}$  (introduced in Sec. II) can be calculated for the 4 atoms in the  $\text{Ni}_4\text{Mo}$ -unit cell as shown in Fig. 4 and Table I. For  $\epsilon$  the value of  $0.063 \pm 0.006 \text{ \AA}$  has been fitted to the experimental data. For several crystallographic directions intensities have been measured at the points indicated in Fig. 5 and the structure factors calculated. The measured intensities have been normalized by structure factors and both (measured O and normalized ▲) have been reported in Fig. 6. The result is, that the normalized intensities can be represented by a simple curve. Moreover this new distorted structure has nearly vanishing structure factors for reflections at  $(\frac{24}{5}, \frac{8}{5}, 0)$  and other points (see Fig. 5) which, indeed, have not been found experimentally, even after an extensive investigation.

Furthermore the normalized points have been fitted to the expression

$$2 \ln [ \lambda \exp(-\sigma_1 Q^2/2) + (1 - \lambda) \exp(-\sigma_2 Q^2/2) ] .$$

This represents an extension of the usual Debye-

TABLE I. Calculation of  $\vec{d}$  for each of the 4 D atoms in the  $\text{Ni}_4\text{Mo}$  unit cell. Each D atom (D1, D2, D3, D4) has three nearest-neighbor vacancies (see Fig. 4). Therefore the three unit vectors  $\vec{d}_1, \vec{d}_2, \vec{d}_3$  directed toward nearest-neighbor vacancies are indicated with their coordinates in columns 2–4.

Atom	$\sqrt{2}\vec{d}_1$	$\sqrt{2}\vec{d}_2$	$\sqrt{2}\vec{d}_3$	$\sqrt{2}\vec{d}$
D1	(0,1,1)	(0,1,-1)	(-1,-1,0)	(-1,1,0)
D2	(-1,1,0)	(1,0,1)	(1,0,-1)	(1,1,0)
D3	(1,-1,0)	(-1,0,1)	(-1,0,-1)	(-1,-1,0)
D4	(1,1,0)	(0,-1,1)	(0,-1,-1)	(1,-1,0)

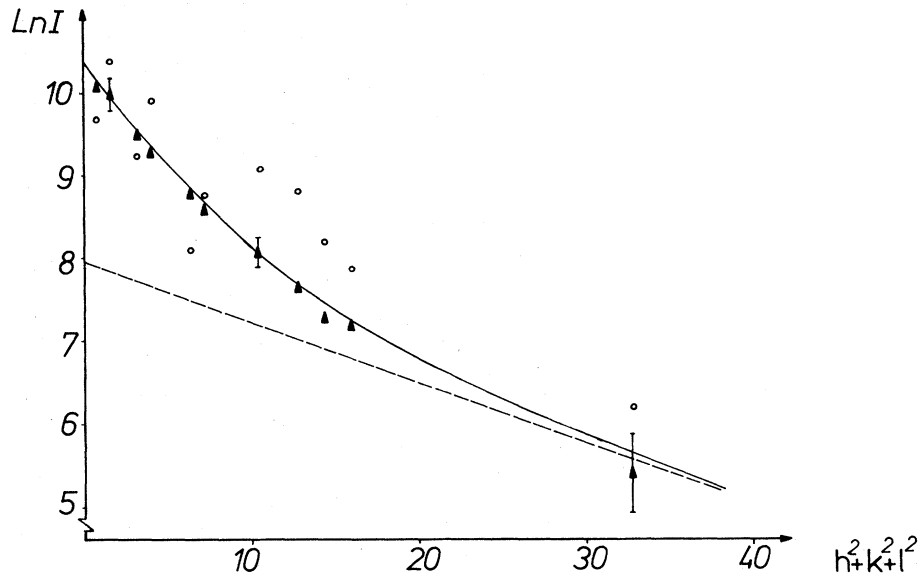


FIG. 6. In a logarithmic scale the measured and normalized intensities of superlattice reflections have been represented (by circles and triangles, respectively) vs  $(a^2/4\pi^2)Q^2 = h^2 + k^2 + l^2$  ( $a$  is the lattice parameter). Full line indicates the calculated curve and broken line the slope corresponding to thermal vibrations.

Waller factor approximation, which would be reobtained for  $\lambda = 1$ . The upper expression can be obtained as follows: The amplitude of the diffracted wave can be written

$$A = K \sum_j \exp[-i\vec{Q} \cdot (\vec{r}_j + \delta\vec{r}_j)] ,$$

where  $\vec{r}_j$  are the mean atom positions (equal to the octahedral site corrected by the distortion described before) and  $\delta\vec{r}_j$  are the differential random positions around the equilibrium. It follows  $A = A_0 \langle e^{-i\vec{Q} \cdot \delta\vec{r}} \rangle$ . Let  $p(\vec{u})$  be the probability for  $\delta\vec{r}$  to be equal  $\vec{u}$ , then

$$\langle e^{-i\vec{Q} \cdot \delta\vec{r}} \rangle = \int_{R^3} p(\vec{u}) e^{-i\vec{Q} \cdot \vec{u}} d\vec{u} = F(p) ,$$

where  $F$  stands for Fourier transformation. Consequently

$$\ln(I/I_0) = \ln\{F(p)[F(p)]^*\} .$$

As the standard distribution for  $p$  would be a Gaussian, therefore  $F(p)$  would be a Gaussian  $e^{-\sigma Q^2/2}$  and  $\ln(I/I_0) = -\sigma Q^2$  which means the linear dependence in  $Q^2$  predicted by the Debye-Waller approximation.

If one chooses for  $p(\vec{u})$  a sum of two Gaussians,

$$p(\vec{u}) = \lambda(2\pi\sigma_1)^{-3/2} \exp\left[-\frac{u^2}{2\sigma_1}\right] + (1-\lambda)(2\pi\sigma_2)^{-3/2} \exp\left[-\frac{u^2}{2\sigma_2}\right] .$$

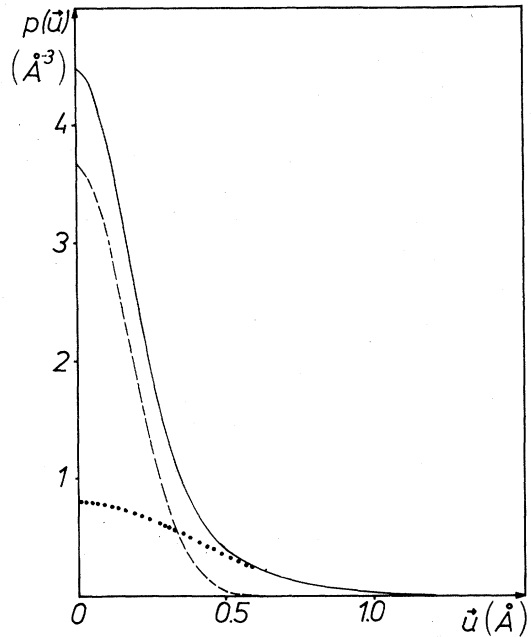


FIG. 7. Full line indicates the fitted distribution  $p$  of a mean D atom around its equilibrium position. Broken line indicates  $p_1$ , the part of  $p$  corresponding to thermal vibrations, and dotted line is the Gaussian  $p_2$ , the remaining part of  $p$ .

It follows by Fourier transformation

$$\ln(I/I_0) = 2 \ln[\lambda e^{-\sigma_1 Q^2/2} + (1-\lambda)e^{-\sigma_2 Q^2/2}]$$

This curve is represented in Fig. 6 with

$$\sigma_1 = 0.030 \text{ \AA}^2, \quad \sigma_2 = 0.146 \text{ \AA}^2, \quad \lambda = 0.3$$

It can be seen that for greater  $Q^2$  the slope is nearly constant and equal to  $-\sigma_1$ . This means that for greater  $Q^2$  the Debye-Waller-factor approximation is valid and one obtains  $\langle u^2 \rangle_1 = 3\sigma_1 = 0.09 \text{ \AA}^2$ , which corresponds to the value for thermal deuterium vibrations already found.<sup>2,6</sup>

The distribution  $p$  is depicted in Fig. 7 together with the two Gaussians  $p_1$  and  $p_2$  of which it is composed.  $p_1$  (broken line) describes the behavior at higher  $Q^2$  and leads to the standard description in terms of thermal Debye-Waller factor. However,  $p_2$  represented with dotted line, is responsible for the rapid decrease of intensity at lower  $Q^2$ . This may indicate the presence of a random static distortion in PdD<sub>x</sub>, but even a dynamic origin cannot be excluded by this method.

#### IV. DISCUSSION

The content of the present paper is centered around two points. (a) A structural model is proposed for the short-range-ordered state which is able to describe the observed diffuse intensity around the  $(1, \frac{1}{2}, 0)$  point in PdD<sub>x</sub> with  $0.71 \leq x \leq 0.78$ . The model describes the short-range order by "mixed" domains consisting of ordered cells of the Ni<sub>n</sub>Mo type. Moreover a simple distortion, i.e., a relaxation of the D atoms towards the vacant site explains the observed intensity asymmetry. (b) The same relaxation of the D atoms towards the vacancy has been introduced in the long-range-ordered Ni<sub>4</sub>Mo structure.

The calculated intensities of the superlattice reflection in this distorted structure are consistent with the measured intensities reported in this paper. Furthermore, the experimental investigations have revealed the presence of a relatively large  $\langle u^2 \rangle$ , when the isotropic  $Q$  dependence of the superlattice intensities is described by a Debye-Waller factor.

In view of these structural models the ordering in PdD<sub>x</sub> with  $0.71 \leq x \leq 0.78$  at low temperatures may be described in the following form. When the temperature is lowered in the region of the "50-K anomaly" the D atoms become ordered in the "mixed" microdomains of the Ni<sub>n</sub>Mo type. The mixed state is favored by the easy local transformation possibility between different Ni<sub>n</sub>Mo structures. At lower concentrations the system remains "frustrated" in the mixed state, at higher concentrations, however, where the Ni<sub>4</sub>Mo structure is favored by its concentration the long-range-ordered structure appears.

The present model for low-temperature ordering in PdD<sub>x</sub> has been based on experimental results found in a concentration range from  $x = 0.71$  to 0.78. We have shown that the model may explain these results. We have not tried to extend the validity of the model to concentrations below  $x = 0.7$ , where the intensity distribution is centered at the  $(1, \frac{1}{2}, 0)$  point and shows a considerable time dependence,<sup>2</sup> i.e., the peak increases in intensity and is narrowing with time so that the observed phenomena are even qualitatively different when compared to those of the high-concentration range.<sup>2</sup>

#### ACKNOWLEDGMENTS

We would like to thank Professor Weinzierl for continuous support. This research was supported in part by "Fonds zur Förderung der wissenschaftlichen Forschung in Österreich."

<sup>1</sup>T. E. Ellis, C. B. Satterthwaite, M. H. Mueller, and T. O. Brun, Phys. Rev. Lett. **42**, 456 (1979).

<sup>2</sup>I. S. Anderson, D. K. Ross, and C. J. Carlile, Phys. Lett. **68A**, 249 (1978).

<sup>3</sup>O. Blaschko, R. Klemencic, P. Weinzierl, O. J. Eder, and P. von Blanckenhagen, Acta Crystallogr. A **36**, 605 (1980).

<sup>4</sup>P. R. Okamoto and G. Thomas, Acta Metall. **19**, 825 (1971).

<sup>5</sup>D. de Fontaine, Acta Metall. **23**, 553 (1975); D. de Fontaine, Solid State Phys. **34**, 73 (1979).

<sup>6</sup>M. H. Mueller, J. Faber, H. E. Flotow, and D. G. Westlake, Acta Crystallogr. A **31**, 599 (1975).